Contact State Estimation using Multiple Model Estimation and Hidden Markov Models

Thomas Debus[1], Pierre Dupont[1], and Robert Howe[2]

[1]Boston University, Boston MA 02215, USA
[2]Harvard University, Cambridge MA 02138, USA

Abstract: This paper presents an approach to estimating the contact state between a robot and its environment during task execution. Contact states are modeled by constraint equations parameterized by time-dependent sensor data and time-independent object properties. At each sampling time, multiple model estimation is used to assess the most likely contact state. The assessment is performed by a Hidden Markov Model, which combines a measure of how well each set of constraint equations fit the sensor data with the probability of specific contact state transitions. The latter is embodied in a task-based contact state network. The approach is illustrated for a three dimensional peg-in-hole insertion using a tabletop manipulator robot. Using only position sensing, the contact state sequence is successfully estimated. Property estimates are obtained for the peg dimensions as well as the hole position and orientation.

1   Introduction

One aspect of machine perception is the automatic determination of contact states and the object properties associated with those states. Such information is useful in a broad range of manipulation problems. For example, in many tasks, the values of object properties (e.g., location, dimensions, mass, stiffness) determine the subsequent handling strategy. The use of such a system for undersea connector mating during oil platform maintenance was explored in [1]. A second category involves those tasks for which the current contact state dictates the motion or control strategy to be applied.

Force controlled assembly represents a class of problems for which knowledge of both contact states and property values is important. The control law depends on the contact state; and accurate knowledge of the geometric parameters improves controller performance. Significant progress for this application has been made by De Schutter et al. [2]. In their approach, contacts between a manipulated object and the environment are modeled as virtual mechanisms whose geometry and nominal parameter values are known. Geometric uncertainties are estimated with Kalman filters using motion data, force data or both. This approach also allows the estimation of contact state.

Our approach assumes that the geometry of possible contact states is known; however, nominal parameter values *are not assumed*. Thus, the contact state of a cylinder sliding on a plane can be distinguished regardless of the cylinder's radius

and an estimate of the unknown radius is also obtained. Without the assumption of nominal contact parameters, however, the estimation problem is nonlinear. In this paper, contact states are described by nonlinear kinematic constraint equations.

The paper is arranged as follows. Section 2 presents an overview of the approach and provides a brief summary of related literature. The following section describes the kinematic contact state models. Section 4 provides the details of the segmentation and estimation algorithms. Experimental results appear in Section 5, which is followed by concluding remarks.

2   Approach

The work described in this paper builds on the framework for a robotic perceptual system first proposed in [3]. The structure of the perceptual system is motivated by three fundamental observations involving contact states, constraints equations, and task descriptions:

- Object properties are measurable only in certain contact states,
- Each contact state can be described by a set of constraint equations, and
- Manipulation tasks are readily described as a succession of contact states.

A variety of modeling approaches have been reported for use in segmenting a sensor data stream by contact state. De Schutter et al. employed Kalman filtering of position and force data to estimate geometric contact uncertainties and used a Bayesian approach to monitor the change of contact state during a peg-in-hole task [2]. Eberman used generalized likelihood ratio tests [4]. McCarragher has employed qualitative reasoning with thresholding [5] as well as Petri nets [6]. Hidden Markov models have also been used. For example, Hannaford and Lee used force and torque signals as the inputs to an HMM to monitor contact states during peg-in-hole insertion [7].

In this paper, contact state estimation is performed by combining multiple model estimation (comparing how well each contact model fits the data) with a Hidden Markov Model (HMM) representation of the robot's task (providing a network of allowable contact states and probabilities of transitions). Our approach is depicted in Fig. 3 with the HMM incorporated in the acceptance test. This approach contrasts with prior use of HMM's in which the HMM input consisted of raw sensor data. Instead, the HMM developed here employs estimation residuals corresponding to object penetration distances for each contact state.

3   Modeling

In this paper, contact states are modeled using their kinematic constraints. The associated properties are the dimensions and locations of objects, all of which can be estimated based on point contact locations. For example, the typical contact states comprising a spatial peg-in-hole insertion are depicted in Fig. 1.
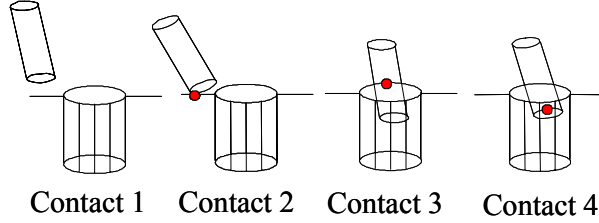
<div align="center">Contact 1   Contact 2   Contact 3   Contact 4</div>

Fig. 1. Peg-in-hole contact states.

3.1 Modeling Contact States Using Position Based Constraint Equations

Each contact state can be expressed using sets of parameterized constraint equations that describe the position of the contact point. For example, in Contact 2, the contact point belongs to the bottom rim of the peg and to a plane in the environment frame. For the general case, constraints on the point contact coordinates can be expressed as

$$
\begin{aligned}
f_j({}_c^m x(t), {}_c^m y(t), {}_c^m z(t)) &= 0 \\
g_j({}_c^e x(t), {}_c^e y(t), {}_c^e z(t)) &= 0
\end{aligned}
\tag{1}
$$

Here, f_j and g_j are vector-valued functions of the contact's coordinates written with respect to body frames of the manipulated object, ${}_c^m X(t) = [{}_c^m x(t), {}_c^m y(t), {}_c^m z(t)]^T$, and the environment object, ${}_c^e X(t) = [{}_c^e x(t), {}_c^e y(t), {}_c^e z(t)]^T$.

These functions are related through the following kinematic closure equation:

$$
{}_o^g T(t)\,{}_g^m T(t)\,{}_c^m X(t) = {}_o^e T(t)\,{}_c^e X(t)
\tag{2}
$$

${}_o^g T(t)$ is a homogeneous transform matrix which relates the gripper frame to the sensor frame based on the geometry of the remote manipulator. Similarly ${}_g^m T(t)$ relates the manipulated object to the gripper frame, and ${}_o^e T(t)$ relates the environment object body frame to the sensor frame.

By substituting the contact constraints (1) into the kinematic closure equation (2) we can express the geometric constraints characterizing the contact states in terms of the sensor measurements and the properties associated with the objects in contact. Techniques from the robot calibration literature, e.g., [8], can be applied to obtain the best form of these equations for estimation.

3.2 Contact equations reformulation as penetration constraints

In the kinematic closure equation, (2), the left and right sides represent the fixed-frame coordinates of the contact point on the manipulated object and on the

environment object, respectively. When the contact constraints (1) are substituted into (2), the equality of the latter holds if the contact state is active and there is no error in the sensor data and in the property estimates. Otherwise, (2) can be modified to obtain a residual vector, ε_0, indicating the error in the closure equation:

$$\varepsilon_o(t) = {}^g_o T(t) {}^m_g T(t) {}^m_c X(t) - {}^e_o T(t) {}^e_c X(t) \tag{3}$$

For those point contacts with a well-defined contact normal, n, the residual vector ε_o can be projected along the normal direction to obtain the distance by which the contact constraint is violated.

$$\varepsilon_p = \varepsilon_0 \cdot n \tag{4}$$

Depending on its sign, the penetration distance ε_p indicates interpenetration of the objects or the distance between them. Fig. 2 shows examples of penetration distance for two contact states of a planar peg-in-hole insertion. As can be expected, the projection of (4) preserves those variables directly associated with the contact constraints while eliminating those that are not. Section 4 explains how penetration distance can be used in contact state and property estimation.
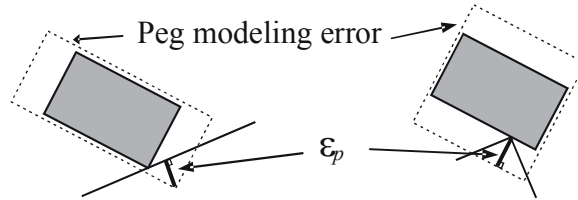
Fig. 2. Penetration distance, due to error modeling, for two contact states of planar peg-in-hole insertion

3.3 Anticipated Path Constraints

To ensure that the unknowns of equation (4) are time-independent, path restrictions are imposed on the estimable motion associated with the different contact states. The assumption is made that, for some portion of a contact state, the operator will follow an anticipated path within that contact state. In Contact 2, for example, the operator is likely to slide the peg without changing the point of contact on the peg for some segment of motion. In this approach, the success of data segmentation and property estimation depends on the operator producing those constrained motions for at least some short time interval during the associated contact states. An example is provided in section 5.2.

4 Contact State and Property Estimation

The technique of simultaneously comparing a set of models to a data stream and using a statistical test to select the model which best fits the data is known as multiple model estimation. Its application to contact state and property estimation is illustrated in Fig. 3. Note that the approach provides a unified solution to the segmentation and the estimation problems.

With this technique, the parameters (properties) of all contact states are estimated simultaneously in a moving data window of fixed length. To implement nonlinear least squares based on penetration distance, the Levenberg-Marquardt algorithm is used since it is robust to the choice of initial parameter values. The condition number of the Jacobian relating parameters to penetration distance is evaluated and those data windows exceeding a threshold are discarded [8]. Finally, the estimation residuals of well-conditioned data windows become the inputs to an acceptance test that provides an estimate of the contact state.
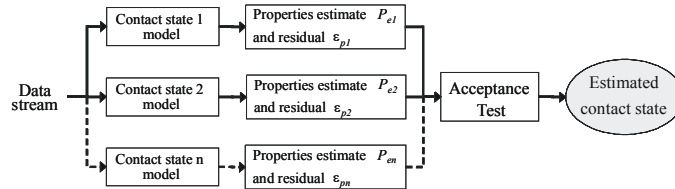

Fig. 3. Multiple model estimation

4.1 Acceptance test by Hidden Markov Model

The acceptance test is implemented with a Hidden Markov Model (HMM). To estimate the contact state of a data window, the HMM uses the estimation residuals, an estimate of the previous contact state and the probability of specific contact state transitions.

An HMM can be described as a probabilistic observer by which a stochastic hidden process can be observed using the probabilistic structure of the state network and a probabilistic relationship between the states and one or several observable stochastic signals. The contact state network of the HMM is described by n, the number of states, ρ, the n-vector of initial state probabilities, and A, the $n \times n$ state transition probability matrix [9].

The probabilistic relationship between the observable signal and the different states that comprise the task network is given by the observation sequence O. For a continuous signal this relationship can be described using a probability density function (pdf), $B(O)$. Gaussians are used here for practicality.

As described in [9], the computation of the estimated sequence of states associated with the observable signal O is a minimization problem that can be efficiently solved using dynamic programming techniques such as the Viterbi algorithm. Once the state sequence is estimated, the object properties parameterizing the contact state constraint equations can be estimated.

4.2 Multi-pass Data Segmentation

Note that while contact state constraints can have some parameters in common (e.g., peg radius appears in contacts 2-4), the estimated values of these common parameters (in $p_{ei}, i = 2\ldots4$ of Fig. 3) can differ as they are determined independently in the multiple model approach. It can be anticipated that these parameters will be well conditioned in some contact states and poorly conditioned in others.

Constraint conditioning can be greatly improved by setting one or more common parameters to their correct values. While the correct values are assumed unknown a priori, a multi-pass approach to segmentation can be implemented to estimate them. This technique is based on segmenting a well-conditioned subset of the contact states on each pass. Estimates of common parameters are used to augment the subset of well-conditioned contact states for the subsequent pass. The technique can successfully segment all contact states if at least one additional state becomes well conditioned with each pass. Note that all passes are performed on the same data set.

5 Experiment results

The proposed contact state and property estimation techniques are implemented for peg-in-hole insertion using a tabletop manipulator system. The goal of the experiment is to estimate the sequence of contact states composing the task and to extract the associated task properties. These properties include the radius and length of the peg as well as the location and orientation of the hole.

5.1 System configuration

A PHANToM® haptic device is used as the manipulating robot. The positions of the six joints of the system are measured using high resolution optical encoders. The kinematics of the robot are known, and a closed loop calibration technique [8] is used to improve the absolute accuracy of the system.

The peg and hole apparatus is constructed as follows. A cylindrical peg is attached through the spherical wrist of the manipulator robot. The hole is drilled perpendicularly to the surface of a rectangular aluminum block that is mounted on a 3-DOF vice. The insertion is done manually, using the manipulating robot as a way of recording the kinematic data.

5.2 Contact equations

As a first step, the position-based constraint equations of (1) need to be written for each contact state. For Contact 2, this can be written as follows:

$$\textit{Contact } 2: \quad {}_{c}^{m}z(t) = 0, \quad {}_{c}^{m}x(t)^2 + {}_{c}^{m}y(t)^2 = R_{peg}^2, \quad {}_{c}^{e}z(t) = 0 \tag{5}$$

Then, to obtain the penetration distance for each contact state, the corresponding

constraint equations are combined with the kinematic closure equation (2) and projected along the contact's surface normal as in (4). For example, in contact 2 of Fig. 1, the peg is constrained to slide on the planar surface. The resulting expression for penetration distance is given by

$$\varepsilon_{p2} = ({}^o_e R \varepsilon_o) \cdot n^z_e = \boldsymbol{H_z cos\beta_1 cos\beta_2 - H_x sin\beta_2 - H_y cos\beta_2 sin\beta_1} +$$
$$\boldsymbol{L_p(cos\beta_2(-q^t_{33}cos\beta_1 + q^t_{23}sin\beta_1) + q^t_{13}sin\beta_2) + R_p cos\alpha(cos\beta_2(-q^t_{31}cos\beta_1 + q^t_{21}sin\beta_1) - q^t_{11}sin\beta_2)} \quad (6)$$
$$\boldsymbol{+R_p sin\alpha(cos\beta_2(-q^t_{32}cos\beta_1 + q^t_{22}sin\beta_1) - q^t_{12}sin\beta_2) + q^t_{14}sin\beta_2 + q^t_{24}cos\beta_2 sin\beta_1 - q^t_{34}cos\beta_1 cos\beta_2}$$

The bolded variables in this equation are the unknown parameters: β_1 and β_2 describe the orientation of the plane; R_p and L_p are the radius and length of the peg; H_x, H_y, H_z describe the hole's center coordinates; and α is the angular coordinate locating the contact point on the rim of the peg. The q_{ij} are functions of the robot's kinematic parameters and joint angles. In the general case, α is time dependent, however, for contact 2, a constant value is assumed as an anticipated path constraint. Note the terms forming the first line of (6) do not multiply any input and so together form a single unknown parameter. Expressions for ε_{p3} and ε_{p4} take a similar form.

5.3 State Network Modeling

Possible transitions between the contact states of figure 1 can be represented by a state network as shown in the figure below. As modeled, all the possible state transitions are represented (i.e., an ergodic model). Each transition is labeled by its transition probability, a_{ij}, from the transition probability matrix A defined in section 4.1. For example, a direct transition from state S_2 to state S_4 is physically impossible and thus, a_{24} is set to zero. Selection of the remaining probability values is discussed in the following section.
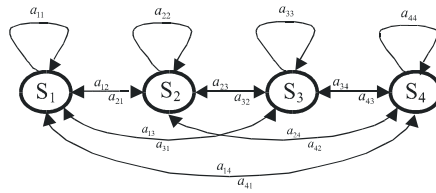

Fig. 4. Contact state network

$$A = \begin{bmatrix} a_{11} & a_{12} & a_{13} & a_{14} \\ a_{21} & a_{22} & a_{23} & a_{34} \\ a_{31} & a_{32} & a_{33} & a_{34} \\ a_{41} & a_{42} & a_{43} & a_{44} \end{bmatrix}$$

$$where \sum_{j=1}^{4} a_{ij} = 1$$

5.4 Contact State and Property Estimation

The multiple model estimation approach of Fig. 3 is used to segment the data stream by contact state. Orientation and position of the robot's tip are recorded at a

7

rate of 25 Hz, and the penetration distances are computed at each time step for contacts 2, 3 and 4. These three distances constitute the observation signal used as the input of a four-state HMM.

To obtain values for the initial probability vector, ρ, probability transition matrix, A, and probability density function, B, defining the HMM, training techniques like as the Baum-Welch algorithm can be used [9]. Such techniques are best suited for applications with large numbers of states, e.g., speech recognition. Since the task under consideration is comprised of only four states, it is possible to assign the HMM parameters manually.

To illustrate the dependence of contact state estimation on parameters of the HMM, figure 5 and 6 compare the output of two models, HMM_{2r} and HMM_{2f}, with manual segmentation. The latter was performed by the operator who pressed a switch at each perceived state transition.

In both cases, the multi-pass estimation strategy described in section 4.2 is used to estimate the different contact states and associated properties during task execution. For peg insertion only two passes are needed. The well-conditioned subset employed in the first pass consists of Contact 2 alone. This contact is selected since it allows for the largest range of peg pitch and yaw angles. Consequently, it provides the best estimates of the common parameters describing peg length, radius and orientation of the hole. The first pass uses a two-state HMM to distinguish between Contact 2 and every other contact state. Results of the first pass estimation is shown in HMM_1 of figure 5 and 6. Estimates of β_1, β_2, R_{peg} and L_{peg} from this pass are used to simplify the constraints of Contacts 3 and 4. The second pass (HMM_2) uses a four-state HMM to distinguish all task contact states.

Figure 5 described the case where the experimental data on which these models were tested corresponds to the most likely (most often observed) sequence of contact states for peg insertion, $\{S_1, S_2, S_3, S_4, S_1\}$. HMM_{2r} assumes the task starts in state S_1 and only permits the most likely transitions. HMM_{2f} accords the largest transition probabilities to the most likely transitions, but also allows all other possible transitions. While this additional flexibility produces two short time segments in which the state is falsely identified for HMM_{2f}, both models successfully match manual segmentation for states 1-4.

Figure 6 illustrates the case when the task involves unexpected state transitions. In that situation the use of a rigid state transition matrix, as shown in HMM_{2r}, results in a poor segmentation of the data set. The state transition matrix can be seen as a weighting matrix of the input signals. Therefore, when an unexpected state sequence occurs, a rigid state transition matrix does not provide enough information to differentiate the different states. This is particularly noticeable when state transitions occur, since it is always expected than a state has a higher probability to stay in its current state than moving to another one. However when

some flexibility is added to the HMM, as shown in HMM_{2f}, the ε_p's combined to the state transition weights provide sufficient information to successfully estimate all the contact states composing the task. Consequently, in order for an HMM to be successful, the input signals (i.e, ε_p) must be discriminatory enough to overcome a potentially low-information transition matrix.
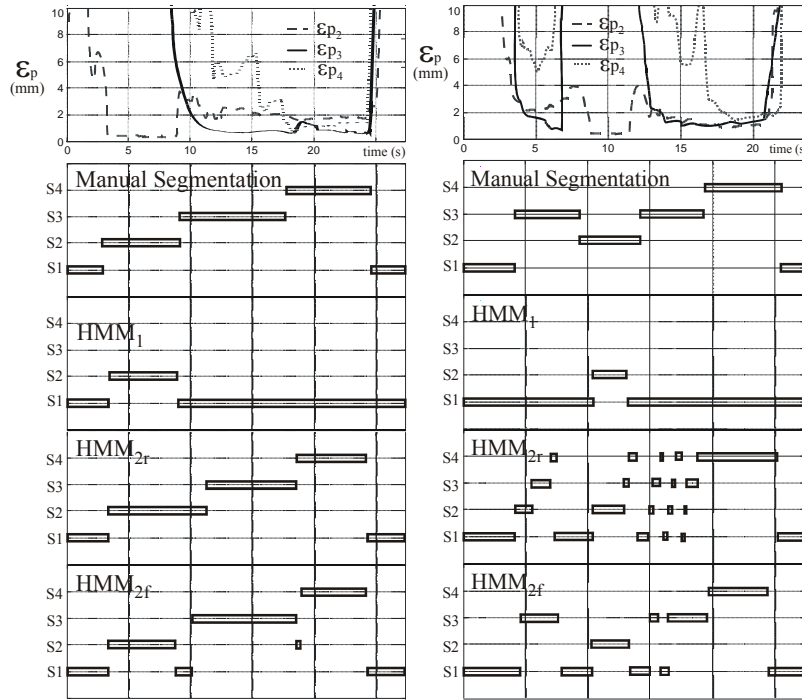
Fig. 5. Segmentation of most likely sequence of task states using HMM.

Fig. 6. Segmentation of unexpected state sequence using HMM

This two-pass technique using a flexible state transition matrix was found to be robust to variations in state sequence. Parameter estimates for a typical trial were found to be within 5 percent of the measured properties. Note that a relatively large ratio of peg to hole diameters (0.98) was employed to facilitate manual segmentation during algorithm development. Automatic segmentation of smaller ratios has also been performed successfully.

6   Conclusion

The combined property and contact state estimation method developed in this paper is based on multiple model estimation using a Hidden Markov model as a decision test. The experimental implementation demonstrates that the algorithm

can successfully estimate various contact state sequences composing a task. Object properties are estimated to a level of accuracy far exceeding what could be achieved by an operator. The only inputs needed by the algorithm are the forward kinematics of the robot, a description of the contact states, and an HMM description of the task to be performed.

The flexibility of the proposed approach makes it straightforward to augment the perceptual capabilities of an existing system. The technique can be easily extended to consider additional sensors (e.g., force) and the estimation of other properties (e.g., inertia, friction). It can also be combined with a linearized approach to estimating contact uncertainties with the former providing initial parameter values for the latter.

Acknowledgements

References

1. Debus, T., Stoll, J., Howe, R. and Dupont, P. (2001). Combined Human and Machine Perception in Teleoperated Assembly. Experimental Robotics VII, D. Rus and S. Singh (Eds.) Springer, New York, 51-60.
2. De Schutter, J., Bruyninckx, H., Dutre, S., De Geeter, J., Katupitiya, J., Demey, S., Lefebvre, T. (1999). Estimating First Order Geometric Parameters and Monitoring Contact Transitions During Force Controlled Compliant Motion. *International Journal of Robotics Research*, 18(12), December, 1161-1184.
3. Dupont, P., Schulteis, T., Millman, P., and Howe, R. (1999). Automatic Identification of Environment Haptic Properties. *PRESENCE: Teleoperators and Virtual Environments*, 8(4), August, 392-409.
4. Eberman, B. (1997). A Model-Based Approach to Cartesian Manipulation Contact Sensing. *International Journal of Robotics Research,* 16(4), August, 508-528.
5. McCarragher, B. J., (1994a). Force Sensing from Human Demonstration Using a Hybrid Dynamical Model and Qualitative Reasoning. *Proceedings of the 1994 IEEE Conference on Robotics and Automation*, 1, May, 557-563.
6. McCarragher, B. J., (1994b). Petri Net Modeling for Robotic Assembly and Trajectory Planning. *IEEE Transactions on Industrial Electronics*, 41(6), December, 631-640.
7. Hannaford, B., and Lee, P. (1991).Hidden Markov Modal Analysis of Force/Torque Information in Telemanipulation. *International Journal of Robotics Research*, 10(5), October, 528-539.
8. Hollerbach, M. J., and Wampler, C. M., (1996). The Calibration Index and Taxonomy for Robot Kinematic Calibration Methods. *International Journal of Robotics Research,* 15(6), December, 573-591.
9. Rabiner, L. R. (1989). A tutorial on hidden Markov models and selected applications in speech recognition. *Proceedings of the IEEE*, 77(2), 257-286.